Self-assembled amphiphilic chitosan nanoparticles for quercetin delivery to breast cancer cells

Rafael de Oliveira Pedro [ab], Stefan Hoffmann [b], Susana Pereira [b], Francisco M. Goycoolea [b,c], Carla C. Schmitt [a], Miguel G. Neumann [a,*]

[a]Instituto de Química de São Carlos, Universidade de São Paulo, Caixa Postal 780, 13560-970 São Carlos, SP, Brazil

[b]Institute of Plant Biology and Biotechnology (IBBP), Westfälische Wilhelms-Universität Münster, Schlossgarten 3, Münster 48149, Germany

[c]School of Food Science and Nutrition, University of Leeds, Leeds LS2 9JT, United Kingdom

E-mail address: neumann@iqsc.usp.br (M.G. Neumann).

ABSTRACT

Novel drug delivery strategies are needed to meet the complex challenges associated to cancer therapy. Biocompatible pH-sensitive drug delivery nanocarriers based on amphiphilic co-polymers seem to be promising for cancer treatment. In the present study, a drug delivery system was produced by encapsulating quercetin into novel pH-sensitive self-assembled amphiphilic chitosan nanoparticles. Up to 83% of quercetin was entrapped by the nanoparticles. The particle diameter, as measured by dynamic light scattering (DLS), ranged from~235 to~312 nm for the blank and~490 to~502 nm for the loaded carriers. The results showed that the payload release is larger at acidic pH (5.0) than at physiological pH (7.4). Fitting the data to the Korsmeyer-Peppas model indicated that anomalous diffusion is the predominant release mechanism at pH 5.0, while Fickian diffusion operates at pH 7.4. The MTT assay revealed that blank nanoparticles were non-antiproliferative for the cell tested. The results further revealed that quercetin maintains its metabolism inhibition against MCF-7 cells after encapsulation. Cellular uptake experiments showed that nanoparticles accumulated on the cell surface, whereas few were internalized. Haemocompatibility test results suggest that the nanoparticles exhibit suitable blood compatibility for biological applications. Results suggest that nanoparticles might be a promising pH-sensitive drug delivery system for applications in anticancer treatment.

1. Introduction

Drug-based therapy is one of the most important strategies in cancer treatment. A major concern in this therapy is to ensure drug selectivity to the target tumour tissue. In chemotherapy, the biodistribution of the drug in healthy regions can cause severe side effects [1]. To overcome this problem, drug delivery systems capable of responding to biological stimuli and promoting selective release in the target area have been developed [2–4]. Drug carriers that respond to pH changes have proven to be suitable for this type of application, since fermentative glycolysis in cancerous tissues generates by-products (lactate and H^+), which lead to acidosis of the extracellular region [5,6]. Recent studies have shown that pH-sensitive carriers based on chitosan can improve the drug bioavailability of formulations intended for cancer therapy due to the biological properties of this polymer [7,8].

Chitosan is a natural polysaccharide obtained from the deacetylation of chitin and formed by 2-acetamide-2-deoxy-D-glucopyranose and2-amino-2-deoxy-D-glucopyranose units. Applications of this polymer can be found in different fields such as agriculture [9], water treatment [10], food [11] and biomedical applications [12]. The versatile use of chitosan in many sectors is due to the presence of functional groups, such as hydroxyls and amines, which confer it with unique physicochemical and biological properties. In line with other biopolymers, chitosan has proven biocompatibility, biodegradability, mucoadhesivity, antimicrobial activity, capacity of reversible opening of tight junctions, and non-immunogenicity [13–17]. These properties have been extensively explored for the

development of chitosan-based drug carrier systems [18–20], thus improving pharmacokinetic and pharmaco dynamic properties of drugs, in addition to controlling their concentration in the body. Chitosan-based nanocarriers can also reduce the toxicity and improve drug selectivity for target cells or tissues in cancer therapy [14,21].

Amphiphilic chitosan derivatives that self-assemble into nanoparticles in aqueous solution can be a good strategy for obtaining carriers. During the process of self-assembly in water, these derivatives generate materials with properties and structures that can only be obtained by this method. Moreover, the structure of the polymer can be chemically modified to give the carrier the ability to respond to bio-logical stimuli such as changes in temperature and pH. Given that the pH of cancerous tumours may be as low as 5.0 [22,23] and that chitosan is protonated at pH below its pKa (~6.4) [24], nanocarriers based on this biopolymer may respond to changes of pH by improving the drug release kinetics in tumour tissues. Protonation may increase the spacing between the chitosan chains that compose the carrier through electrostatic repulsions and hydrogen bonds with water molecules, thus facilitating drug diffusion into the external environment. Furthermore, an important property of biocompatible carriers is its facility to be injected into the bloodstream in order to deliver the drug to the target.

Quercetin (QCT) is a natural flavonoid found in onions, grapes, tomatoes, seeds, nuts and berries [25]. Among the various biological properties of QCT, the anti-oxidative, anti-inflammatory, anti-diabetic and anti-obesity properties are outstanding [25–28]. It also has anti-tumour activity against different cancer types [29]. Some studies have demonstrated that QCT can inhibit cell proliferation by inducing apoptosis and/or cell cycle arrest [29–31]. However, the pharmacological applications of QCT are limited due to its low solubility in water, stability, half-life and bioavailability. Therefore, a strategy for improving the pharmacological properties of QCT and reducing its adverse effects is the use of drug delivery systems such as pH-sensitive carriers based on chitosan [17,32,33]. Carriers cannot only improve the effectiveness of this bioflavonoid, but also enable it to target regions of interest, such as cancerous tissues, by triggering the release at specific pH.

In this study, QCT was loaded into novel pH-sensitive amphiphilic nanoparticles originated by the self-assembling of chitosan modified by hydrophilic and hydrophobic chains grafted to the chitosan backbone, as previously reported by our group [34]. The aim of the present work was to evaluate the suitability of these system as drug carriers. The encapsulation efficiency and release of QCT in vitro was investigated as function of the medium pH. The mathematical model of Korsmeyer–Peppas was applied to the release profiles to get hints on the mechanism of drug release. The colorimetric MTT assay was performed in vitro on a breast cancer cell line (MCF-7) to evaluate the anti-proliferative activity of free QCT, blank nanoparticles and QCT-loaded nanoformulations. Cellular uptake of nanoparticles was performed by confocal laser scanning microscopy. A chitosan-affinity protein fused to a superfolder green fluorescent protein (CAP-sfGFP) was unprecedentedly used to mark the surface of the particles formed by the amphiphilic derivatives of chitosan. Haemolysis tests were performed to verify the hemocompatibility of the nanocarriers.

2. Experimental section

2.1. Materials

Chitosan powder (low molecular weight) was used as received from Sigma-Aldrich Chemical Co., Brazil. QCT, RPMI-1640 cell culture medium, 3-(4,5-dimethylthiazol-2-yl)-2,5-diphenyltetrazolium bromide (MTT) and Pur-A-Lyzer™ Mini Dialysis Kit (MWCO 6–8 kDa) were purchased from Sigma-Aldrich GmbH, Germany. Ultrapure water obtained from a Millipore water purification system (Milli-Q, Millipore GmbH, Germany) was used to prepare aqueous solutions. All chemicals reagents used in the study were analytical grade.

2.2. Amphiphilic chitosan

Amphiphilic chitosan samples were synthesized, characterized and formally reported in our previous study [34]. The hydrophilic group (5-bromopentyl) trimethylammonium bromide (BPTA) and the hydro-phobic group dodecyl aldehyde (DDA) were used as grafting agents. Two amphiphilic samples were previously obtained: $CHP_{40}D^5$ containing 42.2% of the BPTA group and 5.2% of the DDA group and $CHP^{40}D^{30}$ containing 42.2% of BPTA and 33.8% of DDA. Table 1 (reproduced from [34]) summarizes the physical-chemical properties of the amphiphilic samples, including commercial (CHC) and deacetylated (CH) chitosan.

Table 1

Properties of the chitosan derivatives.

Sample	DD[a] (%)	DS$_1$[b] (%)	DS$_2$[c] (%)	M$_v$[d] (kg/mol)
CHC	81.8	—	—	82.3
CH	96.9	—	—	50.4
CHP$_{40}$D$_5$	—	42.2	5.2	—
CHP$_{40}$D$_{30}$	—	42.2	33.8	—

[a]Deacetylation degree determined by[1]H NMR.

[b]Degree of substitution at the hydrophilic chain determined by1H NMR.

[c]Degree of substitution at the hydrophobic chain determined by1H NMR.

[d]Molecular weights determined by viscosimetry (The constants used in the Mark equation were a= 0.76 and K= 0.076 mL/g for CHC and a= 0.82 and K= 0.076 mL/g for CH, as suggested by Rinaudo *et al.* [35]).

2.3. Nanoparticles formation and drug loading

Blank and QCT-loaded nanoparticles were prepared based in a self-assembling process. Amphiphilic samples (20 mg) were dispersed in buffer solution (3 mL, pH 5.0 or 7.4) containing the drug previously solubilized in ethanol (1 mg/mL). The mixture was under gentle stirring protected from light for 12 h at room temperature. Subsequently, the loaded nanoparticles were collected after centrifugation at 10,000g for50 min at 15 °C. UV–visible spectrophotometry at 376 nm was used to measure the free drug concentration in the supernatant [36]. A series of diluted concentrations of QCT solutions in N-N-dimethylformamide (DMF) were prepared to obtain a calibration curve. The entrapment efficiency (EE) and the drug loading efficiency (LE) were calculated using the following equations

$$EE(\%) = \frac{(total\ drug\ weight - free\ drug\ weight)}{(total\ drug\ weight)} \ \text{x}\ 100\% \tag{1}$$

$$LE(\%) = \frac{(total\ drug\ weight - free\ drug\ weight)}{(loaded\ drug\ weight + nanoagreggates\ weight)} \ \text{x}\ 100\% \tag{2}$$

A dynamic light scattering with non-invasive back scattering (DLS-NIBS) at an angle of 173° (Malvern Zetasizer NanoZS) was used to determine the size distribution of the self-assembled nanoparticles at 0.1 g/L and pH 7.4 (phosphate buffer).

2.4. In vitro drug release

The drug release behaviour of the self-assembled nanoparticles was assessed in buffer solutions (pH 5.0 or 7.4) at controlled temperature (37 °C), gentle stirring and absence of light. QCT-loaded nanoparticles previously dispersed in buffer solutions were introduced into a Pur-A-Lyzer™ Mini Dialysis Kit (MWCO 6–8 kDa) and submerged in 35 mL of release medium (respective buffer solutions).

Afterwards, 3 mL aliquots of the release medium were taken at pre-determined intervals and replaced by the same volume of fresh buffer solutions to maintain sink conditions of the media. UV–visible spectrophotometry was used to determine the concentration of the released drug as described above.

2.5. Drug release mechanism modelling

The Korsmeyer–Peppas model (Eq. (3)) is frequently applied to indicate the combined effect of erosion and diffusion mechanisms of drugs in delivery formulations [19,37–40]:

$$\frac{Mt}{M\infty} = Kt^n \tag{3}$$

where M_t is the mass of drug released at time t, M_∞ expresses the total mass of drug to be released and k is a constant related to structural characteristics of the nanoaggregates and the solvent/material interactions. The exponent indicates the type of diffusion. Fickian diffusion occurs when $n = 0.43$, while Case II transport takes place when $n = 0.85$. If n is in between these values, anomalous diffusion is predominant, and if $n > 0.85$ the diffusion comprises super-Case II transport. It is possible to have Fickian diffusion in polydispersed systems based in spherical particles when n is lower than 0.43 [41]. The portions of the release profile where $M_t/M_\infty \leq 0.6$ were employed in the determination of the n exponent.
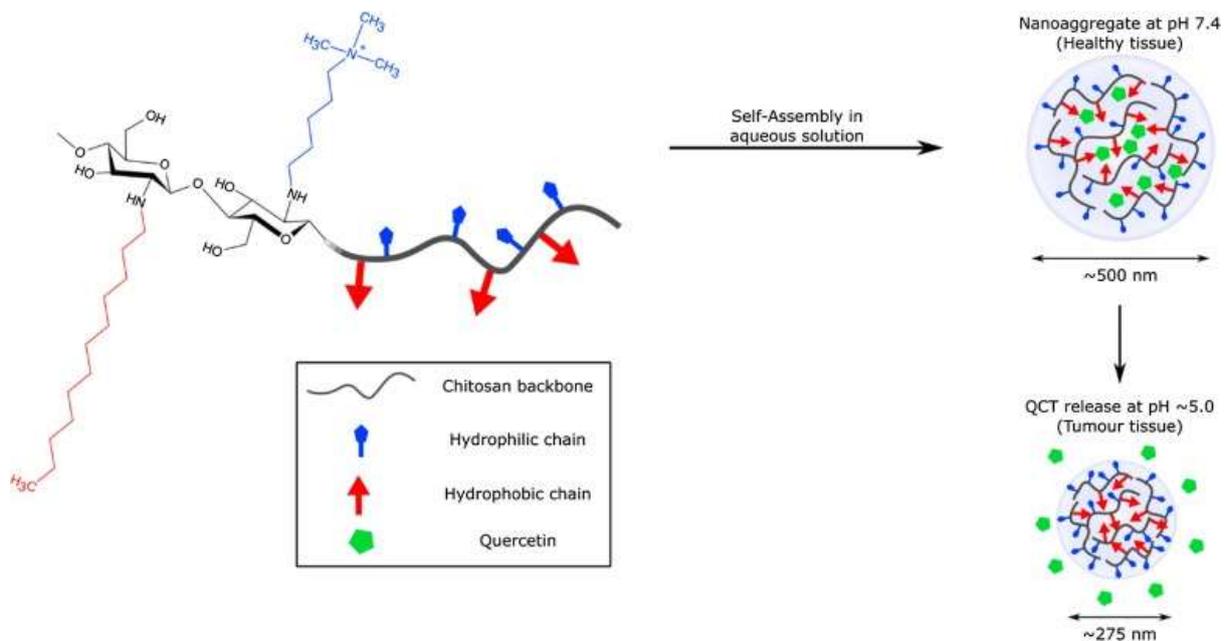
Fig. 1 Schematic representation of self-assembled amphiphilic nanoparticles for targeted delivery of quercetin into cancer cells.

2.6. MTT assay

Colorimetric MTT studies of the free QCT, blank and QCT-loaded nanoparticles were performed in vitro on breast cancer cell line (MCF-7) to assess cell viability. The cells were cultivated in RPMI 1640 medium (Sigma-Aldrich) supplemented with 10% (v/v) fetal bovine serum, 1% (v/v) L-glutamine (200 mM) and 1% (v/v) penicillin-streptomycin (10000 units penicillin, 10,000 units of streptomycin in 0.9% NaCl). 100μL of cell suspension with cellular density of~104cells per well (or~105cells/mL) were added to a 96-well tissue culture plate before incubation for 24 h at 37 °C in 5% CO₂. Afterwards, the cells were washed with supplement-free RPMI 1640 medium and the medium containing the samples was added. After 24 h incubation, the samples were removed, the wells washed twice with supplement-free medium and replaced with 100μL of medium containing 25μL of MTT solution in PBS (5 mg/mL), followed by 4 h of incubation. Subsequently, the medium was carefully removed and 100μL of DMSO were added to each well to solubilize the crystals. After orbital shaking at 300 rpm for 15

min at 37 °C, the absorbance was measured at λ= 570 nm in a microtiter plate reader (Safire, Tecan AG, Salzburg, Austria). Triton X-100(4% (v/v)) in PBS was used as a positive control and negative control cells were incubated with the complete medium. All treatments were tested on eight individual microplate wells and treatments were repeated as independent triplicates on different days. Relative viability is expressed as a percentage of the negative control (Relative cell viability (%) = [Treated cells/Control cells] × 100). Statistical analysis was performed using Student's t-test ($P < 0.05$) to compare the relative viability of the tested formulations with the free QCT. Data were analysed using Prism v6.0c (GraphPad Software Inc., La Jolla, USA).

2.7. Cellular uptake of nanoparticles by confocal laser scanning microscopy

Nanoparticles cell internalization assays were performed using the nanoaggregates formed by the $CHP_{40}D_5$ sample as proof of concept. The aggregates were stained using 100 μg/ml of chitosan-affinity protein fused to a superfolder green fluorescent protein (CAP-sfGFP) that was heterologously expressed and purified as previously described [42,43]. Association efficiency of CAP-sfGFP was assessed in vitro using the microplate reader mentioned previously with excitation wavelength at 470 nm and emission at 510 nm. A calibration curve of CAP-sfGFP up to 0.15 μM was prepared in water. A fixed amount of nanoparticles was mixed with 0.05, 0.10 and 0.15 μM of CAP-sfGP in 1.5 mL reaction tubes. Afterwards, the tubes were centrifuged (10,000g for 45 min at 15 °C) to pellet the nanoparticles and associated CAP-sfGFP. Aliquots of the supernatant containing free CAP-sfGFP were measured against the calibration curve to evaluate the amount of CAP-sfGFP that was associated with the nanoparticles. All measurements were performed in triplicates.

MCF-7 cells were cultured on 8-wellμ-slide plates until confluence. Subsequently, the wells were treated with 100μL of free CAP-sfGFP, blank and CAP-sfGFP-labelled nanoparticles solutions, followed by 1 h of incubation at 37 °C and 5% CO2. Afterwards, the samples were removed and cell membrane was counterstained with CellMask™ Orange Plasma Membrane Stain (Thermo Fisher Scientific). Next, fixation was performed using 4% paraformaldehyde solution and nuclei were stained with HCS CellMask™Red stain (Thermo Fisher Scientific). Staining was carried out according to the supplied protocol. Samples were then immediately observed on a Confocal Laser Scanning Microscope (Leica TCS SP2).

2.8. Blood compatibility

The haemocompatibility of the nanoparticles was carefully checked. Blood was drawn from healthy pigs and diluted with PBS buffer (1:1.25). 20 μL of the diluted blood were added to tubes containing nanoparticles previously dispersed in PBS (1 mL, 1 mg/mL) and incubated for 60 min at 37 °C with gentle agitation. The absorbance of the released haemoglobin was checked using a UV–Vis spectrometer at 545 nm. The haemolysis ratio (HR) was calculated using

$$HR\ (\%) = \frac{A_{sample} - A_{PBS}}{A_{water} - A_{PBS}} \times 100\% \tag{4}$$

where A_{sample}, A_{PBS} and A_{water} are the absorbance at 545 nm of blood samples containing nanoparticles, PBS (negative control) and water (positive control), respectively. All experiments were carried out in triplicate.

3. Results and discussion

3.1. Nanoparticles formation and QCT encapsulation

As reported previously [34], the nanoparticles (Table 1) from amphiphilic derivatized chitosan are spontaneously formed by a self-assembling process (Fig. 1). These amphiphilic particles were studied herein as drug carriers using QCT as a model drug.

The size of blank and QCT-loaded nanoparticles were evaluated by DLS. The average diameter of the $CHP_{40}D_5$ chitosan increased from 235 ± 22 to 490 ± 18 nm after QCT encapsulation, while the nanoparticles formed by $CHP_{40}D_{30}$ increased from 312 ± 35 to 502 ± 33 nm. These average diameters are in accordance with studies reported in the literature using other self-assembling chitosan derivatives [44–46].

The core of the nanoparticles is formed by hydrophobic alkyl chains, which allows interaction with hydrophobic molecules such as QCT. Once the nanoparticles are obtained by the aggregation of the individual polymer chains, it is also possible that some hydrophobic micro domains may remain in the outer layer due to the conformation of the chitosan. Therefore, QCT will be placed mainly within the aggregates, but may also be present at the surface of the nanoparticles. This characteristic is probably responsible for the effective interaction with the drug, as observed by the encapsulation efficiency results (Table 2). The entrapment efficiency gives information about the amount of drug that was successfully encapsulated, while the drug loading indicates the drug content of the isolated nanoparticles.

The results shown in Table 2, suggest that the amount of hydrophobic substitution (DS) of the samples, as well as the pH can affect the EE and LE. It appears that an increase in hydrophobic content (from 5 to 33% in the samples $CHP_{40}D_5$ and $CHP_{40}D_{30}$, respectively) tends to increase the amount of QCT encapsulated by the nanoaggregates due to the existence of more sites for the interaction with the drug. It is also interesting to note the influence of pH on the encapsulation efficiency. Due to the protonation of the residual amine groups of chitosan at pH 5.0, more water molecules participate in the formation of hydrogen bonding with the polymer. The electrostatic repulsion between the positive charges of the protonated amine groups also contributes significantly to increase the spacing between the chains [24]. Thus, allowing the formation of aggregates with expanded core, which facilitates the interaction of the drug with the internal portion of the particles. On the other hand, at pH 7.4, due to the deprotonation of the residual amines, the formation of aggregates with more condensed core restricts the drug access to the hydrophobic chains of the polymer. This behaviour was observed by Xiong *et al.* [47] for chitosan nanoparticles containing *Auricularia auricula* polysaccharide, which has been documented with promising potential in biomedical and food applications. When the pH increased from 3.0 to 6.0, the average nanoparticles sizes decreased from 310 to 278 nm. Therefore, it is possible to use pH to control the amount of QCT that will be entrapped by the nanoparticles.

Table 2

Characteristics of the quercetin-loaded nanoaggregates (*n*= 3, mean values ± SD).

Sample	pH	EE[a] (%)	LE[b] (%)
$CHP_{40}D_5$	5.0	71 ± 7	4.3 ± 0.4
	7.4	18 ± 1	1.1 ± 0.1
$CHP_{40}D_{30}$	5.0	83 ± 8	4.9 ± 0.6
	7.4	21 ± 2	1.3 ± 0.3

[a] Entrapment efficiency.

[b] Drug loading efficiency.

3.2. Quercetin release

Studies of QCT release were performed in buffer solutions (pH 5.0and 7.4). These pHs were chosen to simulate the physiological and tumour tissue conditions (pH 5.0 and 7.4, respectively), since the cancer cell metabolism changes the concentration of H^+ ions in the tumour microenvironment, leading to a more acidic pH than that of the surrounding healthy tissue [22,23,48]. In addition, acidic pH could be found by nanoparticles upon uptake, inside tumour cells in endosomes and lysosomes [49]. It can be

seen that the QCT release process from the $CHP_{40}D_5$ and $CHP_{40}D_{30}$ nanoaggregates proceeds in two stages (Fig. 2). QCT weakly associated to nanoparticles was rapidly released during the first hours, under a phenomenon known as a burst release. Subsequently, the release occurred at a slower and a more sustained rate.

As can be noticed in Fig. 2, pH has a major role in the release process. For both samples the release is more pronounced at pH 5.0 than at 7.4. To account for this, it is suggested that protonation of the residual amine groups of chitosan at pH 5.0 allows the formation of hydrogen bonds with water molecules and promoting electrostatic repulsion between chains, thus causing an expansion of the polymer chains, facilitating the drug diffusion to the external medium. By contrast, the aggregates are more condensed at pH 7.4, where the protonation of residual amino groups is minimal, thus restricting the diffusion process. This behaviour is ideal for cancer drug delivery applications, since the release should be minimal at physiological pH, and reach its maximum in the region of the more acidic pH tumour tissues.

It is important to notice that the degree of hydrophobicity/hydrophilicity of both studied amphiphilic derivatives appears to have little influence on the QCT release process from the nanoaggregates (Fig. 2a and b). The less hydrophobic sample ($CHP_{40}D_5$) reached slightly higher values in the cumulative release when compared to the more hydrophobic derivative ($CHP_{40}D_{30}$) at both pHs. This is probably related to the stronger interactions between the hydrophobic chains and the QCT in the $CHP_{40}D_{30}$ aggregate, which decreases the release. These results are in agreement with the encapsulation efficiency and size determination experiments, indicating that the increase of the hydrophobic content in the chitosan structure seems to lead to the formation of denser aggregates and stronger interactions with QCT, affecting the release.

The calculated fitting parameters of the Korsmeyer-Peppas model after applying a non-linear regression analysis are summarized in Table 3. Interestingly, the data were better adjusted for the releases at pH 5.0 than 7.4, as evaluated by R^2- values. The poor fitting release data achieved at pH 7.4 for both samples suggests that release is substantially hampered by the restrictions to diffusion at this pH, consequently. This result also confirms the role of the pH in the release, once it strongly indicates that the surface area of the particles and the release mechanism change as function of pH due to protonation/deprotonation effect. Thus, the coefficient *n* indicates that at pH 5.0 the anomalous diffusion is predominant while at pH 7.4 the Fickian diffusion occurs.
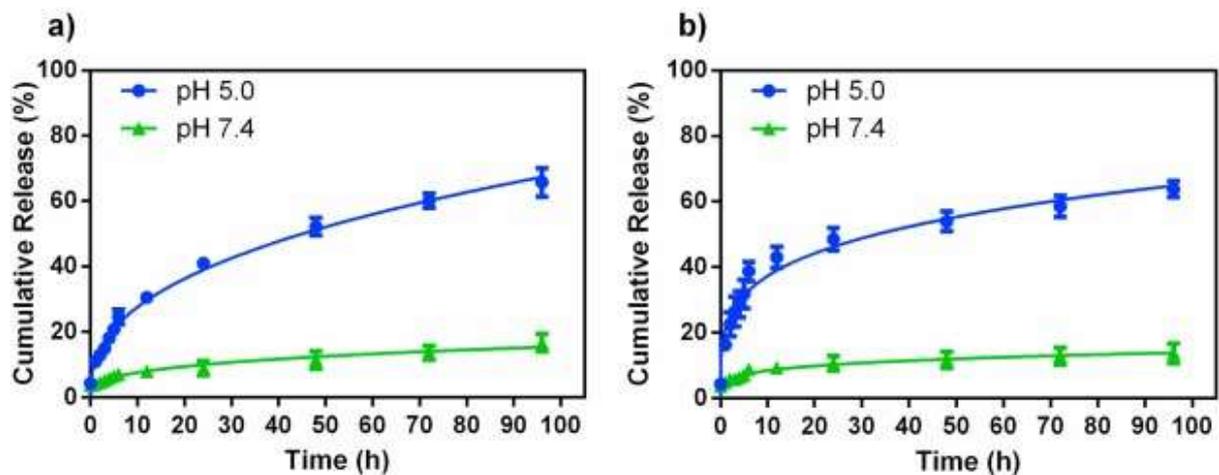
Fig. 2 *In vitro* release profile of QCT from (a) $CHP_{40}D_5$ and (b) $CHP_{40}D_{30}$ at pH 5.0 and 7.4 and at 37 °C.

Table 3

Mathematical parameters of the release data fitting.

Sample	pH	k	n	Correlation coefficient (R^2)	Release mechanism
$CHP_{40}D_5$	5.0	9.3 ± 1.6	0.51 ± 0.11	0.9914	Anomalous difussion
	7.4	4.1 ± 1.3	0.32 ± 0.22	0.9035	Fickian diffusion
$CHP_{40}D_{30}$					
	5.0	15.8 ± 1.7	0.47 ± 0.08	0.9616	Anomalous difussion
	7.4	4.5 ± 1.4	0.32 ± 0.02	0.8529	Fickian diffusion

3.3. MTT assay

The MTT experiments were carried out to evaluate the mitochondrial activity, thus the cell viability, of MCF-7 breast cancer cells upon treatment with free QCT and chitosan carriers. The effects of blank nanoparticles on cell viability were compared (Fig. 3). It can be noted that practically no dose dependent reduction was observed for blank nanocarriers. Another important aspect is that, even at higher concentrations (25 and 50 μg/mL), these particles did not reduce cell viability to less than 84% for the cells tested. These results suggest that the carriers formed by the amphiphilic chitosan derivatives do not significantly affect the cellular metabolism over a 24 h period.

Fig. 3 also shows a comparison between the cell viability of free QCT and QCT-loaded nanoparticles. A dose-response trend can be observed for all samples. The more hydrophobic drug-loaded formulation (QCT-loaded $CHP_{40}D_{30}$) was less efficient in reducing cell viability than the less hydrophobic formulation (QCT-loaded $CHP_{40}D_5$). This effect can be attributed to the difference in the nature of the core of both derivatives. Thus, the $CHP_{40}D_{30}$ nanoaggregates comprised by more hydrophobic chains are bound to establish stronger interaction with the drug, which hinders the release and restricts the therapeutic effect. On the other hand, the $CHP_{40}D_5$ sample showed cell viability comparable to quercetin, being more effective in cellular inhibition at concentrations of 0.1 and 25 μg/mL.
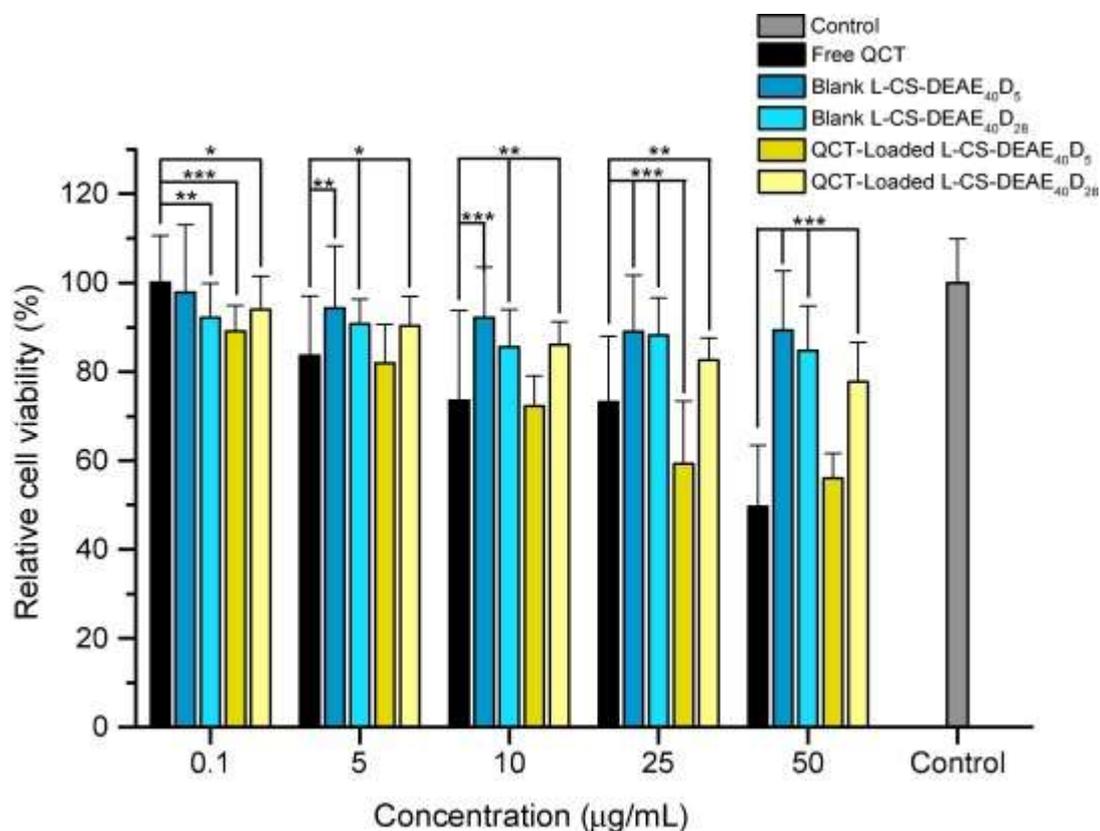
Fig. 3 Variation of the relative cell viability of MCF-7 cells, as determined by the MTT assay, with concentration of free quercetin (QCT), blank nanoparticles formed by amphiphilic chitosans ($CHP_{40}D_5$ or $CHP_{40}D_{30}$) and quercetin-loaded nanoparticles (QCT-loaded $CHP_{40}D_5$ or QCT-loaded $CHP_{40}D_{30}$). Absolute concentrations applied refer to concentration of QCT. For all experiments, cells were incubated for 24 h in 96-well plates (Mean values ± SD, $n = 3$, *** $p < 0.001$).

It is also important to highlight that QCT has to be released from the particles before it affects the cells. This observation is sustained by the results of the release experiments, which revealed that after 24 h (cell incubation time) only a fraction of QCT was released. Furthermore, the cell viability results for QCT-loaded formulations are in good keeping with previously reported ones. According to Duo *et al.* [50], QCT decreases the proliferation and induces apoptosis of MCF-7 cells. The results further revealed that the incubation time of the cells with QCT is directly related to the reduction of cell viability, which suggests that a higher incubation time would have led to higher toxicity. In addition, recent studies have confirmed the bioavailability and effectiveness of QCT against MCF-7 cells [7,51,52].

In conclusion, our *in vitro* studies suggest that QCT maintains its metabolism inhibition activity even after encapsulation in chitosan particles. As a result, loading QCT into nanoparticles might decrease its side effects upon systematic administration due to targeted release in the acidic tumour microenvironment compared to the free drug. Although *in vivo* studies are required to support this observation, the nanocarriers' behaviour and the efficacy of QCT suggest that the systems developed in this study may be further used as a new methodology for the treatment of tumour tissues.

3.4. Cellular uptake of nanoparticles by confocal laser scanning microscopy

Fluorescent proteins have become an important non-destructive and non-invasive tool for studying many phenomena in living cells [53,54]. As proof of concept, chitosan-affinity protein fused to a superfolder green fluorescent protein (CAP-sfGFP) was used as a specific surface biomarker of the nanoparticles derived from CHP40D5. It is worth mentioning that the use of CAP-sfGFP aims to mark the particles in mild conditions, while trying not to significantly change the physicochemical properties of the carrier. The association efficiencies of CAP-sfGFP with the nanoparticles are shown in Table 4.

Table 4

Association efficiencies determined for nanoparticles with CAP-sfGFP (n=3, mean values ± SD).

CAP-sfGFP added to nanosystem [μM]	Supernatant CAP-sfGFP concentration after centrifugation [μM]	Binding efficiency [%]
0.05	0.032 ± 0.003	36.7 ± 5.9
0.10	0.057 ± 0.001	43.3 ± 1.5
0.15	0.106 ± 0.016	29.5 ± 10.8

Association efficiencies of nanoparticles with CAP-sfGFP ranged from~37 to~29%, depending on the initial concentration of CAP-sfGFP. Whereas 0.05 μM and 0.10 μM concentrations of CAP-sfGFP yielded relatively high associations, at the higher concentration (0.15 μM) the association was lower with a higher standard deviation, potentially indicating a saturation of the available binding sites. This may be considered quite interesting in view that the modification of the chitosan might have rendered previously available binding sites unsuitable for CAP binding. To our knowledge, this is the first use of CAP-sfGFP to stain chemically modified chitosans. Due to the large amounts of non-associated CAP-sfGFP for microscopy, control experiments of free CAP-sfGFP with cells were performed.

To facilitate visualization of the particles localization, the membrane and the cell nucleus were stained in orange and red, respectively. Fig. 4a shows that free CAP-sfGFP did not interact with cells, confirming that the fluorescent protein does not have affinity for cellular structures. On the other hand, green fluorescence was observed in the cells treated with nanoparticles (Fig. 4b). Labelled nanoparticles accumulated on the cell surface (blue arrows), whereas others were internalized (red arrows) during the assessment period (Fig. 4c). The direct physical interaction between the nanoparticles and the cell surface is likely to result in a significant increase of the drug in the extracellular microenvironment, which allows the enhancement of the therapeutic effect. In addition, the internalization of the nanoaggregates does allow the drug release directly into the intracellular environment. Additional studies might provide a better understanding of the cellular uptake. Studies using non-linear vibrational spectroscopy are in progress and might provide information on the mechanism of nanoparticles internalization.

3.5. Blood compatibility

In vitro erythrocyte-induced haemolysis can provide preliminary information on the haemocompatibility of the nanoparticles. Previous studies confirmed that the haemolysis test is reliable and extensively used to estimate the blood compatibility of the chitosan nanoparticles. Li *et al*. [55] have shown that *N,O*-carboxymethyl chitosan/oxidized alginate hydrogel has good compatibility. Lauroyl sulphated chitosan has been proved to have suitable haemocompatibility for biological applications [56]. Therefore, the hemocompatibility of nanoparticles formed by amphiphilic chitosan derivatives was preliminary evaluated by a simple spectroscopy method. For $CHP_{40}D_5$ and $CHP_{40}D_{30}$ chitosan nanoparticles incubated with blood, the erythrocyte haemolysis ratio was found to be 3.2 ± 1.8 and 3.5 ± 1.2, respectively. These results prove that haemolysis ratios are below the safety limit of 5%, suggesting that the samples have suitable haemocompatibility for biological applications [57]. In principle, higher haemolysis ratios were expected since it is well known that chitosan has haemolytic tendency [58–60] as a result of electrostatic interactions between the positive charges of chitosan and the negative charges of the cell membranes. This unexpected high haemocompatibility might arise from the presence of the DDA groups, which probably reduce the nanoparticles surface charges. The influence of the alkyl groups has already been reported in the literature. For instance, amphiphilic chitosan derivatives with improved haemocompatibility were obtained using octaldehyde as the hydrophobic reagent [61]. The results also indicate that samples with different degrees of alkyl chain substitution showed similar haemolysis.

The protein adsorption layer formed on the surface of the nanoparticles, also known as the "protein corona", might also be responsible for the improved haemocompatibility of the amphiphilic derivatives [62]. It is well known that surfaces of nanoparticles, especially charged ones, are modified by the adsorption of biomolecules, leading to formation of corona [63]. Upon the intravenous administration, several biomolecules compete to adsorb on the surface of the nanoparticles, increasing its blood compatibility. Furthermore, the opsonisation of nanoparticles by serum or plasma proteins (opsonins) might also affect the final effect on blood [21]. Thus, the preliminary results suggest that the nanoparticles have suitable blood compatibility for biological applications.

4. Conclusion

The present study aimed to develop a novel QCT delivery system based on a pH-sensitive amphiphilic chitosan. The results showed that nanoparticles formed by self-assembly of the modified chitosans can encapsulate up to 83% of the drug. The QCT release is higher at acidic pH (5.0) than at physiological pH (7.4). DLS measurements showed that the particle size range from 235 to 312 nm and 490 to 502 nm for the blank and loaded nanoparticles, respectively. The Korsmeyer-Peppas model was fitted to experimental data and the predominant release mechanism are anomalous diffusion (pH 5.0) and Fickian diffusion (pH7.4). The colorimetric MTT assay showed that blank nanoparticles did not reduce cell viability of the tested cells. The QCT-loaded nanoparticles formed by the $CHP_{40}D_5$ sample exhibited

inhibition effect against MCF-7 comparable to free quercetin, despite having released only a fraction of the drug during the incubation period. The fluorescent protein CAP-sfGFP was used for the first time to stain the surface of particles formed by modified chitosan once incubated with the cells. Cellular uptake experiments performed by confocal laser scanning microscopy showed that CAP-sfGFP-labelled nanoparticles accumulated on the cell membrane, whereas others were internalized. *In vitro* erythrocyte-induced haemolysis results suggest that the nanoparticles have suitable blood compatibility for biological applications.

Thus, the pH-sensitive QCT-loaded nanoparticles might be appropriate for the treatment of breast cancer. Moreover, the carriers may further help in reducing the side effects of QCT, enhancing its biodisponibility and improving its efficacy in treating tumours. Finally, the self-assembling nanoparticles could be used as a drug delivery system for other hydrophobic drugs.
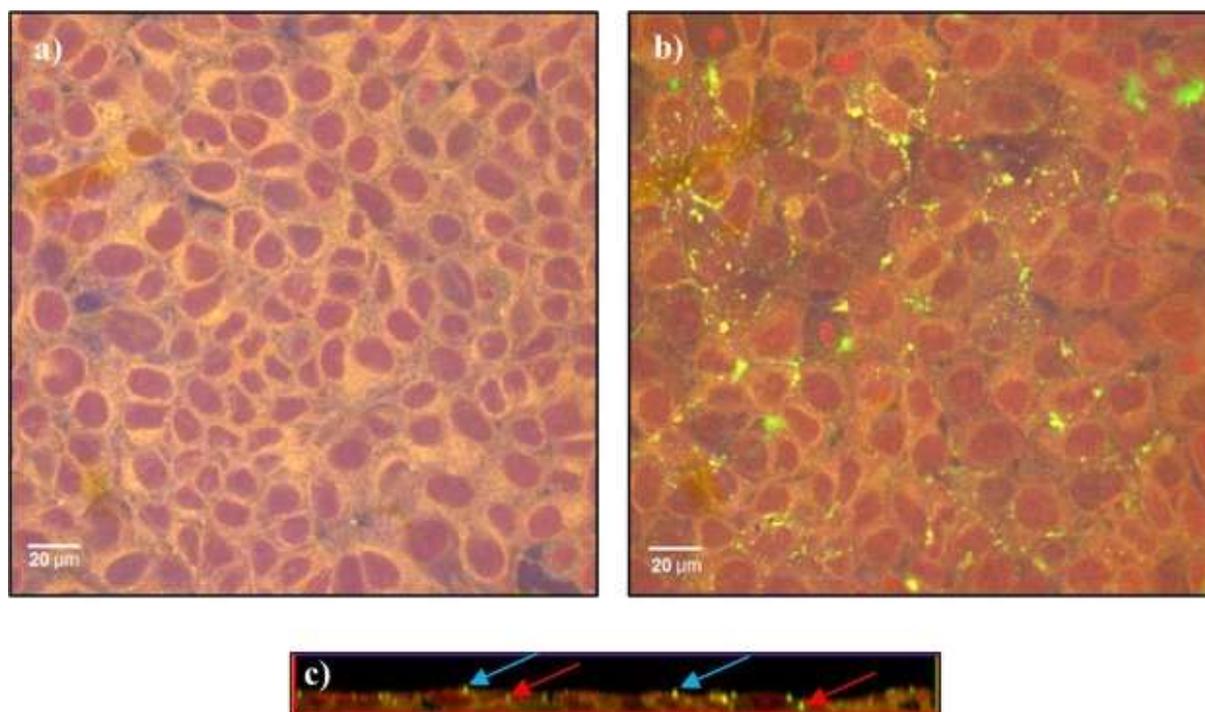
Fig. 4 Representative confocal laser scanning microscopy images of MCF-7 cells incubated during 1 h at 37 °C. (a) Cells incubated with free CAP-sfGFP. (b) Cells incubated with nanoparticles coated with CAP-sfGFP. (c) Vertical section of cells incubated with nanoparticles coated with CAP-sfGFP. Arrows represent nanoparticles interacting with the cell surface (blue arrows) and internalized (red arrows). (For interpretation of the references to colour in this figure legend, the reader is referred to the web version of this article.)

References

[1] S. Roy, G. Trinchieri, Microbiota: a key orchestrator of cancer therapy, Nat. Rev.Cancer 17 (2017) 271–285.

[2] M.E. Davis, Z. (Georgia) Chen, D.M. Shin, Nanoparticle therapeutics: an emerging treatment modality for cancer, Nat. Rev. Drug Discov. 7 (2008) 771–782.

[3] E. Vlassi, A. Papagiannopoulos, S. Pispas, Amphiphilic poly (2-oxazoline) copolymers as self-assembled carriers for drug delivery applications, Eur. Polym. J. 88(2017) 516–523.

[4] D. Xiong, N. Yao, H. Gu, J. Wang, L. Zhang, Stimuli-responsive shell cross-linked micelles from amphiphilic four-arm star copolymers as potential nanocarriers for "pH/redox-triggered"anticancer drug release, Polymer (Guildf) 114 (2017)161–172.

[5] M. Damaghi, J.W. Wojtkowiak, R.J. Gillies, pH sensing and regulation in cancer, Front. Physiol. 4 (2013) 370.

[6] P. Vaupel, F. Kallinowski, P. Okunieff, Bloodflow, oxygen and nutrient supply, and metabolic microenvironment of human tumors: a review, Cancer Res. 49 (1989)6449–6465.

[7] R. de Oliveira Pedro, F.M. Goycoolea, S. Pereira, C.C. Schmitt, M.G. Neumann, Synergistic effect of quercetin and pH-responsive DEAE-chitosan carriers as drug delivery system for breast cancer treatment, Int. J. Biol. Macromol. 106 (2018)579–586.

[8] H. Yang, C. Tang, C. Yin, Estrone-modified pH-sensitive glycol chitosan nanoparticles for drug delivery in breast cancer, Acta Biomater. 73 (2018) 400–411.

[9] A.E.S. Pereira, P.M. Silva, J.L. Oliveira, H.C. Oliveira, L.F. Fraceto, Chitosan nanoparticles as carrier systems for the plant growth hormone gibberellic acid, Colloids Surf. B Biointerfaces 150 (2017) 141–152.

[10] Y.-H. Zhang, F.-Q. Liu, C.-Q. Zhu, X.-P. Zhang, M.-M. Wei, F.-H. Wang, C. Ling, A.-M. Li, Multifold enhanced synergistic removal of nickel and phosphate by a (N, Fe)-dual-functional bio-sorbent: Mechanism and application, J. Hazard. Mater. 329(2017) 290–298.

[11] J.K. Rutz, C.D. Borges, R.C. Zambiazi, M.M. Crizel-Cardozo, L.S. Kuck,C.P.Z. Noreña, Microencapsulation of palm oil by complex coacervation for application in food systems, Food Chem. 220 (2017) 59–66.

[12] A. Anitha, S. Sowmya, P.T.S. Kumar, S. Deepthi, K.P. Chennazhi, H. Ehrlich, M. Tsurkan, R. Jayakumar, Chitin and chitosan in selected biomedical applications, Prog. Polym. Sci. 39 (2014) 1644–1667.

[13] T. Kean, M. Thanou, Biodegradation, biodistribution and toxicity of chitosan, Adv.Drug Deliv. Rev. 62 (2010) 3–11.

[14] A. Kumar, A. Vimal, A. Kumar, Why Chitosan? From properties to perspective of mucosal drug delivery, Int. J. Biol. Macromol. 91 (2016) 615–622.

[15] M.N. Ravi Kumar, A review of chitin and chitosan applications, React. Funct. Polym. 46 (2000) 1–27.

[16] M. Larsson, W.-C. Huang, M.-H. Hsiao, Y.-J. Wang, M. Nydén, S.-H. Chiou, D.-M. Liu, Biomedical applications and colloidal properties of amphiphilically modified chitosan hybrids, Prog. Polym. Sci. 38 (2013) 1307–1328.

[17] J.J. Wang, Z.W. Zeng, R.Z. Xiao, T. Xie, G.L. Zhou, X.R. Zhan, S.L. Wang, Recent advances of chitosan nanoparticles as drug carriers, Int. J. Nanomed. 6 (2011)765–774.

[18] M.N.V.R. Kumar, R.A.A. Muzzarelli, C. Muzzarelli, H. Sashiwa, A.J. Domb, Chitosan chemistry and pharmaceutical perspectives, Chem. Rev. 104 (2004) 6017–6084.

[19] P.I.P. Soares, A.I. Sousa, J.C. Silva, I.M.M. Ferreira, C.M.M. Novo, J.P. Borges, Chitosan-based nanoparticles as drug delivery systems for doxorubicin: optimization and modelling, Carbohydr. Polym. 147 (2016) 304–312.

[20] M. Liu, J. Zhang, X. Zhu, W. Shan, L. Li, J. Zhong, Z. Zhang, Y. Huang, Efficient mucus permeation and tight junction opening by dissociable "mucus-inert" agent coated trimethyl chitosan nanoparticles for oral insulin delivery, J. Control. Release222 (2016) 67–77.

[21] G.D. Mogoşanu, A.M. Grumezescu, C. Bejenaru, L.E. Bejenaru, Polymeric protective agents for nanoparticles in drug delivery and targeting, Int. J. Pharm. 510 (2016)419–429.

[22] E.R. Gillies, T.B. Jonsson, J.M.J. Fréchet, Stimuli-responsive supramolecular assemblies of linear-dendritic copolymers, J. Am. Chem. Soc. 126 (2004)11936–11943.

[23] I.F. Tannock, D. Rotin, Acid pH in tumors and its potential for therapeutic exploitation, Cancer Res. 49 (1989) 4373–4384.

[24] M. Rinaudo, Chitin and chitosan: properties and applications, Prog. Polym. Sci. 31(2006) 603–632.

[25] I. Erlund, Review of the flavonoids quercetin, hesperetin, and naringenin. Dietary sources, bioactivities, bioavailability, and epidemiology, Nutr. Res. 24 (2004)851–874.

[26] N.C. Cook, S. Samman, Flavonoids—chemistry, metabolism, cardioprotective effects, and dietary sources, J. Nutr. Biochem. 7 (1996) 66–76.

[27] S.F. Nabavi, G.L. Russo, M. Daglia, S.M. Nabavi, Role of quercetin as an alternative for obesity treatment: you are what you eat!, Food Chem. 179 (2015) 305–310.

[28] M. Vessal, M. Hemmati, M. Vasei, Antidiabetic effects of quercetin in streptozocin-induced diabetic rats, Comp. Biochem. Physiol. Part C Toxicol. Pharmacol. 135(2003) 357–364.

[29] S. Srivastava, R.R. Somasagara, M. Hegde, M. Nishana, S.K. Tadi, M. Srivastava, B. Choudhary, S.C. Raghavan, Quercetin, a natural flavonoid interacts with DNA, arrests cell cycle and causes tumor regression by activating mitochondrial pathway of apoptosis, Sci. Rep. 6 (2016) 24049.

[30] D. Catanzaro, E. Ragazzi, C. Vianello, L. Caparrotta, M. Montopoli, Effect of quercetin on cell cycle and cyclin expression in ovarian carcinoma and osteosarcoma cell lines, Nat. Prod. Commun. 10 (2015) 1365–1368.

[31] H.-C. Pan, Q. Jiang, Y. Yu, J.-P. Mei, Y.-K. Cui, W.-J. Zhao, Quercetin promotes cell apoptosis and inhibits the expression of MMP-9 and fibronectin via the AKT and ERK signalling pathways in human glioma cells, Neurochem. Int. 80 (2015) 60–71.

[32] C. Chen, J.-L. Zhou, X. Han, F. Song, X.-L. Wang, Y.-Z. Wang, A prodrug strategy based on chitosan for efficient intracellular anticancer drug delivery, Nanotechnology 25 (2014) 255101.

[33] Z. Yuying, Y. Yan, T. Kai, H. Xing, Z. Guolin, Physicochemical characterization and antioxidant activity of quercetin-loaded chitosan nanoparticles, J. Appl. Polym. Sci.107 (2007) 891–897.

[34] R. De Oliveira Pedro, C.C. Schmitt, M.G. Neumann, Syntheses and characterization of amphiphilic quaternary ammonium chitosan derivatives, Carbohydr. Polym. 147(2016) 97–103.

[35] M. Rinaudo, M. Milas, P. Le Dung, Characterization of chitosan. Influence of ionic strength and degree of acetylation on chain expansion, Int. J. Biol. Macromol. 15(1993) 281–285.

[36] H. Du, M. Liu, X. Yang, G. Zhai, The role of glycyrrhetinic acid modification on preparation and evaluation of quercetin-loaded chitosan-based self-aggregates, J. Colloid Interface Sci. 460 (2015) 87–96.

[37] P. Costa, J.M. Sousa Lobo, Modeling and comparison of dissolution profiles, Eur. J. Pharm. Sci. 13 (2001) 123–133.

[38] M. Kaiser, B. Kirsch, H. Hauser, D. Schneider, I. Seuß-Baum, F.M. Goycoolea, In Vitro and Sensory Evaluation of Capsaicin-Loaded Nanoformulations, PLoS One. 10(2015) e0141017.

[39] R.W. Korsmeyer, R. Gurny, E. Doelker, P. Buri, N.A. Peppas, Mechanisms of solute release from porous hydrophilic polymers, Int. J. Pharm. 15 (1983) 25–35.

[40] P. Sriamornsak, N. Thirawong, Y. Weerapol, J. Nunthanid, S. Sungthongjeen, Swelling and erosion of pectin matrix tablets and their impact on drug release behavior, Eur. J. Pharm. Biopharm. 67 (2007) 211–219.

[41] P.L. Ritger, N.A. Peppas, A simple equation for description of solute release I. Fickian and non-fickian release from non-swellable devices in the form of slabs, spheres, cylinders or discs, J. Control. Release. 5 (1987) 23–36.

[42] J.P. Fuenzalida, T. Weikert, S. Hoffmann, C. Vila-Sanjurjo, B.M. Moerschbacher, F.M. Goycoolea, S. Kolkenbrock, Affinity protein-based FRET tools for cellular tracking of chitosan nanoparticles and determination of the polymer degree of acetylation, Biomacromolecules 15 (2014) 2532–2539.

[43] M. Nampally, B.M. Moerschbacher, S. Kolkenbrock, Fusion of a novel genetically engineered chitosan affinity protein and green fluorescent protein for specific detection of chitosan in vitro and in situ, Appl. Environ. Microbiol. 78 (2012)3114–3119.

[44] H.F.G. Barbosa, A.M.F. Lima, S.R. Taboga, J.C. Fernandes, V.A.O. Tiera, M.J. Tiera, Synthesis and self-assembly study of zwitterionic amphiphilic derivatives of chitosan, J. Appl. Polym. Sci. 133 (2016).

[45] H. Du, X. Yang, X. Pang, G. Zhai, The synthesis, self-assembling, and biocompatibility of a novel O-carboxymethyl chitosan cholate decorated with glycyrrhetinic acid, Carbohydr. Polym. 111 (2014) 753–761.

[46] J. Tian, S. Xu, H. Deng, X. Song, X. Li, J. Chen, F. Cao, B. Li, Fabrication of self-assembled chitosan-dispersed LDL nanoparticles for drug delivery with a one-step green method, Int. J. Pharm. 517 (2017) 25–34.

[47] W. Xiong, Q. Zhang, F. Yin, S. Yu, T. Ye, W. Pan, X. Yang, Auricularia auricular polysaccharide-low molecular weight chitosan polyelectrolyte complex nanoparticles: preparation and characterization, Asian J. Pharm. Sci. 11 (2016)439–448.

[48] M.A.C. Stuart, W.T.S. Huck, J. Genzer, M. Müller, C. Ober, M. Stamm, G.B. Sukhorukov, I. Szleifer, V.V. Tsukruk, M. Urban, F. Winnik, S. Zauscher, I. Luzinov, S. Minko, Emerging applications of stimuli-responsive polymer materials, Nat. Mater. 9 (2010) 101.

[49] L. Eun-Kyung, H. Yong-Min, Y. Jaemoon, L. Kwangyeol, S. Jin-Suck, H. Seungjoo, pH-triggered drug-releasing magnetic nanoparticles for cancer therapy guided by molecular imaging by MRI, Adv. Mater. 23 (2011) 2436–2442.

[50] J. Duo, G.-G. Ying, G.-W. Wang, L. Zhang, Quercetin inhibits human breast cancer cell proliferation and induces apoptosis via Bcl-2 and Bax regulation, Mol. Med. Rep. 5 (2012) 1453–1456.

[51] R. de O. Pedro, S. Pereira, F.M. Goycoolea, C.C. Schmitt, M.G. Neumann, Self-aggregated nanoparticles of N-dodecyl, N'-glycidyl (chitosan) as pH-responsive drug delivery systems for quercetin, J. Appl. Polym. Sci. 135 (2018) 45678.

[52] A. Sarkar, S. Ghosh, S. Chowdhury, B. Pandey, P.C. Sil, Targeted delivery of quercetin loaded mesoporous silica nanoparticles to the breast cancer cells, Biochim. Biophys. Acta–Gen. Subj. 2016 (1860) 2065–2075.

[53] J. Chu, Y.-H. Oh, A. Sens, N. Ataie, H. Dana, J.J. Macklin, T. Laviv, E.S. Welf, K.M. Dean, F. Zhang, B.B. Kim, C.T. Tang, M. Hu, M.A. Baird, M.W. Davidson, M.A. Kay, R. Fiolka, R. Yasuda, D.S. Kim, H.-L.

Ng, M.Z. Lin, A bright cyan-excitable orange fluorescent protein facilitates dual-emission microscopy and enhances bio-luminescence imaging in vivo, Nat. Biotechnol. 34 (2016) 760–767.

[54] A. Wagh, S.Y. Qian, B. Law, Development of biocompatible polymeric nanoparticles for in vivo NIR and FRET imaging, Bioconjug. Chem. 23 (2012) 981–992.

[55] X. Li, X. Kong, Z. Zhang, K. Nan, L. Li, X. Wang, H. Chen, Cytotoxicity and biocompatibility evaluation of N, O-carboxymethyl chitosan/oxidized alginate hydrogel for drug delivery application, Int. J. Biol. Macromol. 50 (2012) 1299–1305.

[56] R. Shelma, C.P. Sharma, Development of lauroyl sulfated chitosan for enhancing hemocompatibility of chitosan, Colloids Surf. B. Biointerfaces. 84 (2011) 561–570.

[57] ASTM F756-17, Standard Practice for Assessment of Hemolytic Properties of Materials, 2017.

[58] P. Baldrick, The safety of chitosan as a pharmaceutical excipient, Regul. Toxicol. Pharmacol. 56(2010) 290–299.

[59] S. Mathews, K. Kaladhar, C.P. Sharma, Cell mimetic monolayer supported chitosan-haemocompatibility studies, J. Biomed. Mater. Res. Part A 79A (2006)147–152.

[60] P. Xu, G. Bajaj, T. Shugg, W.G. Van Alstine, Y. Yeo, Zwitterionic chitosan derivatives for pH-sensitive stealth coating, Biomacromolecules 11 (2010) 2352–.

[61] M. Huo, Y. Zhang, J. Zhou, A. Zou, D. Yu, Y. Wu, J. Li, H. Li, Synthesis and characterization of low-toxic amphiphilic chitosan derivatives and their application as micelle carrier for antitumor drug, Int. J. Pharm. 394 (2010) 162–173.

[62] P. del Pino, B. Pelaz, Q. Zhang, P. Maffre, G.U. Nienhaus, W.J. Parak, Protein corona formation around nanoparticles from the past to the future, Mater. Horizons 1(2014) 301–313.

[63] M.P. Monopoli, D. Walczyk, A. Campbell, G. Elia, I. Lynch, F. Baldelli Bombelli, K.A. Dawson, Physical–chemical aspects of protein corona: relevance to in vitro and in vivo biological impacts of nanoparticles, J. Am. Chem. Soc. 133 (2011)2525–2534.